Journal of Colloid and Interface Science 461 (2016) 64–68

Contents lists available at ScienceDirect

Journal of Colloid and Interface Science

journal homepage: www.elsevier.com/locate/jcis

Possible mechanism of structural incorporation of Al into diatomite during the deposition process I. Via a condensation reaction of hydroxyl groups

Dong Liu [a,b], Wenbin Yu [a,b,c], Liangliang Deng [a,b,c], Weiwei Yuan [a,b,c], Lingya Ma [a,b,c], Peng Yuan [a,b,*], Peixin Du [a,b,c], Hongping He [a,b]

[a] CAS Key Laboratory of Mineralogy and Metallogeny, Guangzhou Institute of Geochemistry, Chinese Academy of Sciences, Guangzhou 510640, China
[b] Guangdong Provincial Key Laboratory of Mineral Physics and Materials, Wushan, Guangzhou 510640, China
[c] Graduate School of Chinese Academy of Sciences, Beijing 100049, China

GRAPHICAL ABSTRACT

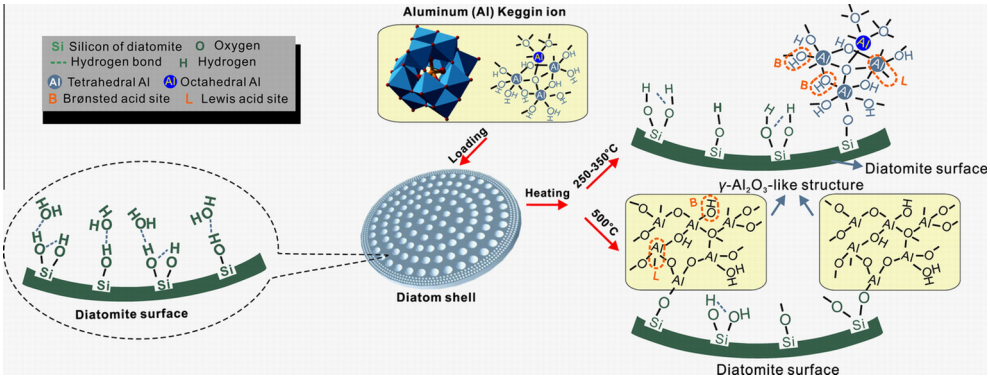

ARTICLE INFO

Article history:
Received 7 July 2015
Revised 23 August 2015
Accepted 24 August 2015
Available online 28 August 2015

Keywords:
Al incorporation
Diatomite
Al_{13}
Solid acidity

ABSTRACT

The structural incorporation of aluminium (Al) into diatomite is investigated by preparing several Al–diatomite composites by loading an Al precursor, hydroxyl aluminum polymer (Al_{13}), onto the surface of diatomite and heating at various temperatures. The results indicate that Al was incorporated and implanted into the structure of diatomite by the condensation reaction of the hydroxyl groups of Al_{13} and diatomite, and the Si–O–Al(OH) groups were formed during the condensation reaction. Al incorporation by the condensation reaction of hydroxyl groups of Al_{13} with single silanols of diatomite occurred more readily than that with geminal silanols. The Al incorporation increased solid acidity of diatomite after Al incorporation. The acidity improvement was various for different types of acid sites, depending on the preparation temperature of the Al-incorporated diatomite. Both Brønsted and Lewis acid sites increased greatly after heating at 250 and 350 °C, but only L acid sites significantly improved after heating at 500 °C. These results demonstrate that the structural incorporation of Al^{3+} ions into diatomite can occur by the condensation reaction of the hydroxyl groups of the Al precursors and diatomite. Moreover, the rich solid acid sites of Al-incorporated diatomite show its promising application as a solid acid catalyst.

* Corresponding author at: Guangzhou Institute of Geochemistry, Chinese Academy of Sciences, Wushan, Guangzhou 510640, China.
E-mail address: yuanpeng@gig.ac.cn (P. Yuan).

http://dx.doi.org/10.1016/j.jcis.2015.08.058
0021-9797/

1. Introduction

Diatomite, also known as diatomaceous earth or kieselguhr, arises from the assemblage of the mineralized exoskeletons of diatoms, which have various macroporous structures with pore sizes extending from the nanometric to the micrometric domains [1,2]. Diatomite is primarily composed of amorphous hydrated silica ($SiO_2 \cdot nH_2O$), which is categorized as non-crystalline Opal-A, according to the mineralogical classification [3,4]. Diatomite is easily obtained at very low cost and has many unique physical and chemical characteristics, enabling their wide uses in a variety of applications for high-performance technologies; thus and widely utilized [5–8,2,9–12].

Aluminum (Al) also exists in diatomite in addition to other major elements of silicon (Si) and oxygen (O). Because the existence of Al in the structure of diatomite is demonstrated to effectively lower the solubility of diatomaceous silica and is beneficial to the preservation of diatomite [13–17], many studies focus on the properties of structural Al in diatomite, such as its content and coordination number (tetrahedral or octahedral coordination) [18–22]. In addition, researchers have estimated the transport of Al from the oceans' surface to the sediment [23–25] by studying the structural Al in diatomite. This is an effective estimator because the Al/Si ratio can be as high as 0.16 [14,15,26], and the diatomaceous earth form is the most abundant form of silica on earth [27].

The existence of Al in the structure of diatomite affects the structure and surface properties. For example, the size of the nano-silica balls, which are the basic components of the diatom shell [28,29,2], most likely changes with the presence of Al in their framework because of the different sizes of Al and Si. In addition, the surface charge and solid acidity vary before and after Al incorporation into the structure [1,9]. However, the effect of Al incorporation on the structure and surface properties has not been investigated.

Moreover, the uptake of structural Al into diatomite is believed to contribute to the biological uptake by living diatoms [30,31,14,32,33,22] and the post-mortem enrichment during the digenetic process [26,22,34]. For the former, Al uptake of diatoms during frustule biosynthesis does not exceed 0.8%, even when the diatoms are grown in high Al concentrations [24,33]. For the latter, previous studies have shown the Al incorporation into the framework of diatomite by mimicking the deposition process of the diatom shell at the sediment–water interface [26,22,34]. A new aluminosilicate phase might form during the process and coat the surface of the diatom frustules [22]. However, to best of our knowledge, no definitive mechanism of Al incorporation into the diatomite framework has been provided.

In this study, hydroxyl aluminium polymer (Al_{13}) was loaded onto the surface of diatomite, and then the obtained composition was heated to various temperatures to incorporate Al into the structure of diatomaceous silica. Detection of the incorporation was performed by combining X-ray diffraction (XRD), solid-state nuclear magnetic resonance (NMR) and Fourier transform infrared spectroscopy (FTIR) to investigate the feasibility and possible mechanism of structural incorporation of Al into diatomite as well as the effect of Al incorporation on the solid acidity of diatomite.

2. Materials and methods

2.1. Diatomite

Diatomite (CAS: 6179053-2) was purchased from Sigma–Aldrich, Inc., which was sourced from the diatomite mine of Jilin Province, China. The dominant diatoms in the diatomite were of the genus *Coscinodiscus* Ehrenberg (Centrales) and were disk-shaped, with a highly developed macroporous structure. The diatomite samples were denoted as Dt (for the morphology, chemical compositions and porosity, see the Supplementary Data).

2.2. Preparation of Al-incorporated diatomite and measurement of solid acidity

Al-incorporated diatomite was prepared as follows. The tridecameric aluminium polymer $[AlO_4Al_{12}(OH)_{24}(H_2O)_{12}]^{7+}$ (aluminium chlorohydroxide solutions, named Al_{13}; for details see the Supplementary Data) was loaded onto the surface of the diatomite, and then the obtained diatomite–Al_{13} composite was heated. Heating was performed in a programmable temperature-controlled muffle oven at 250, 350 and 500 °C for 3 h. The obtained samples were ground into powder in an agate mortar and denoted as Dt/Al_{250}, Dt/Al_{350} and Dt/Al_{500}, respectively. The morphology and macroporous structure of the diatomite remained intact after Al_{13} loading and heating (see the Supplementary Data, Fig. S1).

NH_3 adsorption was performed at room temperature. Approximately 0.3 g of diatomite and Al-incorporated diatomite was spread on the bottom of a ceramic crucible to form a thin layer and was evacuated for 1 h. NH_3 was then slowly introduced and maintained airtight for 48 h. Then, the samples were heated at 120 °C for 1 h under vacuum to remove the physically adsorbed NH_3. The resulting NH_3-adsorbed samples were denoted as Dt-NH_3, Dt/Al_{250}-NH_3, Dt/Al_{350}-NH_3 and Dt/Al_{500}-NH_3. Moreover, the re-adsorption of NH_3 was carried out for KBr pellets prepared by KBr and NH_3-adsorbed diatomite or Al-incorporated diatomite followed by the above processes before FTIR analysis. The NH_3 re-adsorption was to avoid the replacement of NH_3 by water during the preparation of KBr pellets.

2.3. Characterization

The XRD patterns were obtained using a Bruker D8 Advance diffractometer with a Ni filter and Cu Kα radiation ($\lambda = 0.154$ nm) using a generator voltage of 40 kV, a generator current of 40 mA, and a scan rate of 1° (2θ)/min.

The solid-state NMR experiments were performed at $B_0 = 9.4$ T on a Bruker AVANCE III 400 WB spectrometer. The corresponding resonance frequency of ^{29}Si was 79.5 MHz. The samples were packed in a 7 mm ZrO_2 rotor and spun at the magic angle (54.7°) with a spinning rate of 7 kHz. ^{29}Si MAS NMR spectra were acquired using a 90° pulse of 6.0 ls and a recycle delay of 60 s. The ^{29}Si chemical shift was referenced to kaolinite at 91.5 ppm.

FTIR spectra were obtained using the KBr pressed pellet method with a Bruker VERTEX 70 Fourier transform infrared spectrometer. The KBr pellets were prepared by pressing the mixtures of 0.9 mg powder and 80 mg KBr. All of the spectra were collected at room temperature using 64 scans over the range of 4000–400 cm^{-1} with a resolution of 4 cm^{-1}.

3. Results and discussion

3.1. Al incorporation into the diatomite structure

3.1.1. XRD

The XRD pattern of Dt (Fig. 1) is characteristic of one broad reflection centred at approximately 22.5° (2θ), which is in good agreement with that of the reference amorphous Opal-A [10]. A wide and asymmetrical shoulder reflection is displayed in the XRD pattern of Dt and is centred at approximately 6.5° (2θ) (Fig. 1). The reflection is attributed to the clay minerals attached to the surface of diatomite. Note that it is difficult to attribute the reflection to one (or more than one) specific clay mineral(s)

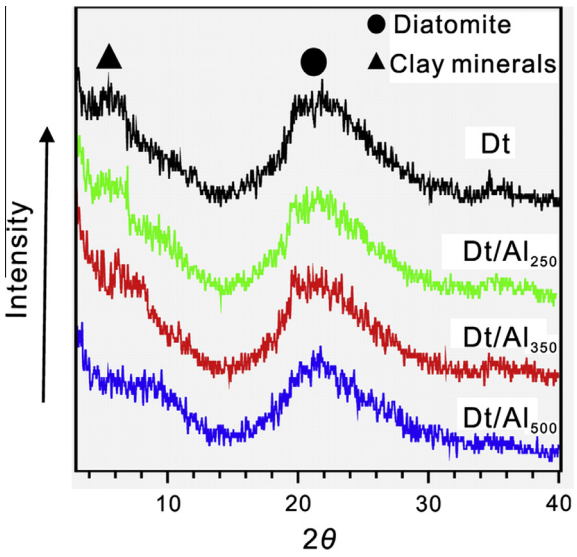

Fig. 1. XRD patterns of Dt and its Al-incorporated products.

based on only one characteristic reflection. The clay minerals impurity, however, is also contained in Dt, which is proved by the reflection, although its quantity is small (<5 wt.%, based on a semi-quantitative calculation). After Al incorporation of diatomite at various temperatures, no evident difference in the 22.5° reflection was observed, and no new reflection appeared, indicating that the framework structure of diatomaceous silica is well maintained and that no new crystallized mineral is formed during Al incorporation of diatomite. Note that Al_{13} should transform into γ-alumina (γ-Al_2O_3) after heating at 500 °C and should show broad and weak characteristic reflections, as reported by studies in the literature [35–37]. However, the typical reflection of γ-Al_2O_3, similar to the result of Al_{13} pillared interlayered clay [37], cannot be observed in the calcined composition of Al_{13} and diatomite (Dt–Al_{500}), which was because only the γ-Al_2O_3 microcrystals, rather than well-crystallized γ-Al_2O_3 particles were formed. Moreover, the *d* spacing of the 6.5° reflection decreases from 1.6 nm for Dt to 1.0 nm for Dt–Al_{500}, which is due to the desorption of interlayer water in the clay minerals or deconstruction of clay minerals.

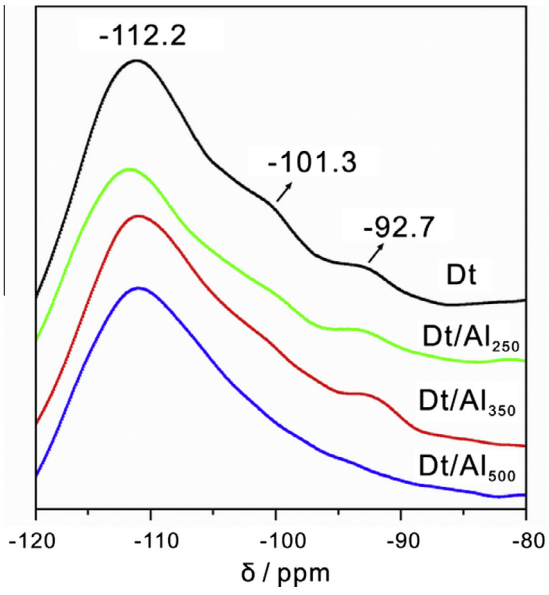

Fig. 2. ^{29}Si MAS NMR spectra of Dt and its Al-incorporated products.

3.1.2. ^{29}Si MAS NMR spectra

The chemical shift signals of the ^{29}Si MAS NMR spectrum of Dt at −112.2, −101.3, and −92.7 ppm (Fig. 2) are assigned to the siloxane bridge ($Si(OSi)_4$), single silanols ($Si(OSi)_3(OH)$), and the geminal silanol ($Si(OSi)_2(OH)_2$) of diatomaceous silica, respectively [12]. The signal of the $Si(OSi)_4$ group is much stronger than the others, showing a predominant formation among all of the silicon groups of Dt. The weak shoulder peaks of the single and geminal silanols imply that their amounts are small, which is consistent with the results in our previous study.

After Al_{13} loading and subsequent heating from 250 to 500 °C, the signal of the $Si(OSi)_3(OH)$ group is gradually weakened and cannot be distinguished in the Dt/Al_{500} sample (Fig. 2). However, blank tests without Al_{13} loading reveal that heating at these temperatures does not affect the group (see Supplementary Data, Fig. S2). In this case, the decrease of the signal is attributed to the condensation reaction of the hydroxyl groups of Al_{13} and diatomite. In addition, the heating temperature affects the condensation reaction, indicating that for higher temperatures, an increased number of single silanols of diatomite reacted with Al_{13} hydroxyl groups. Note that no new signal attributed to the products of the condensation reactions appears, which is due to the low product amount and its signal overlapping with those of other silicon groups. Moreover, the signal shift of another silicon of diatomaceous silica, the geminal silanol ($Si(OSi)_2(OH)_2$), shifts higher; however, the peak pattern after Al_{13} loading and heating at 250 and 350 °C and the relative area of the signal display no evident changes. The nearly complete disappearance of the signal shift occurs after Al loading and heating at 500 °C, indicating that the condensation reaction of the hydroxyl groups of Al_{13} with single silanols is substantially more difficult than that with geminal silanols.

Based on these fundamental results, one possible mechanism for the structural incorporation of Al^{3+} ions into diatomite is attributed to the condensation reaction of hydroxyl groups, which is proposed in this study for the first time. Therefore, the structural Al in natural diatomite is demonstrated as sourced from the post-mortem enrichment of Al, except for the biological uptake by living diatoms.

3.1.3. IR

The bands at 1103, 470, and 800 cm^{-1} in the Dt spectrum are attributed to in-plane Si–O stretching, Si–O–Si deformation, and symmetric Si–O stretching of diatomite, respectively [38,39,12]. In addition, the weak shoulder band at 3745 cm^{-1} is assigned to the isolated O–H stretching of diatomite [12]. The bands at 3420 and 1630 cm^{-1} are attributed to the O–H stretching and deformation of adsorbed water on the Dt surface [38], respectively. Moreover, the bands at 3625 and 910 cm^{-1} in the Dt spectrum are assigned to the O–H stretching and deformation vibrations of the clay minerals attached to the surface of diatomite, respectively, and the 536 cm^{-1} band is attributed to the Si–O–Al vibration of the clay mineral impurity [40]. The clay mineral bands are weak, indicating that only a few clay minerals are attached to the surface of diatomite.

The intensity of the O–H band at 3745 cm^{-1} decreased, as observed in the spectra of Dt/Al_{250} and Dt/Al_{350}, which is attributed to the condensation reaction of the O–H groups on the surface of diatomite and those of Al_{13}. This result shows good agreement with the ^{29}Si MAS NMR spectrum. A new weak shoulder band appears at approximately 745 cm^{-1} in the spectrum (Fig. 3a, insert) of Dt/Al_{250} obtained by Al loading and then heating at 250 °C. This new band is attributed to the Si–O–Al vibration of the Si–O–Al-OH sourced from the condensation of Si-OHs from diatomite and Al-OHs from Al_{13} during 250 °C heating [41]. The absence of the 745 cm^{-1} vibration band provides evidence that

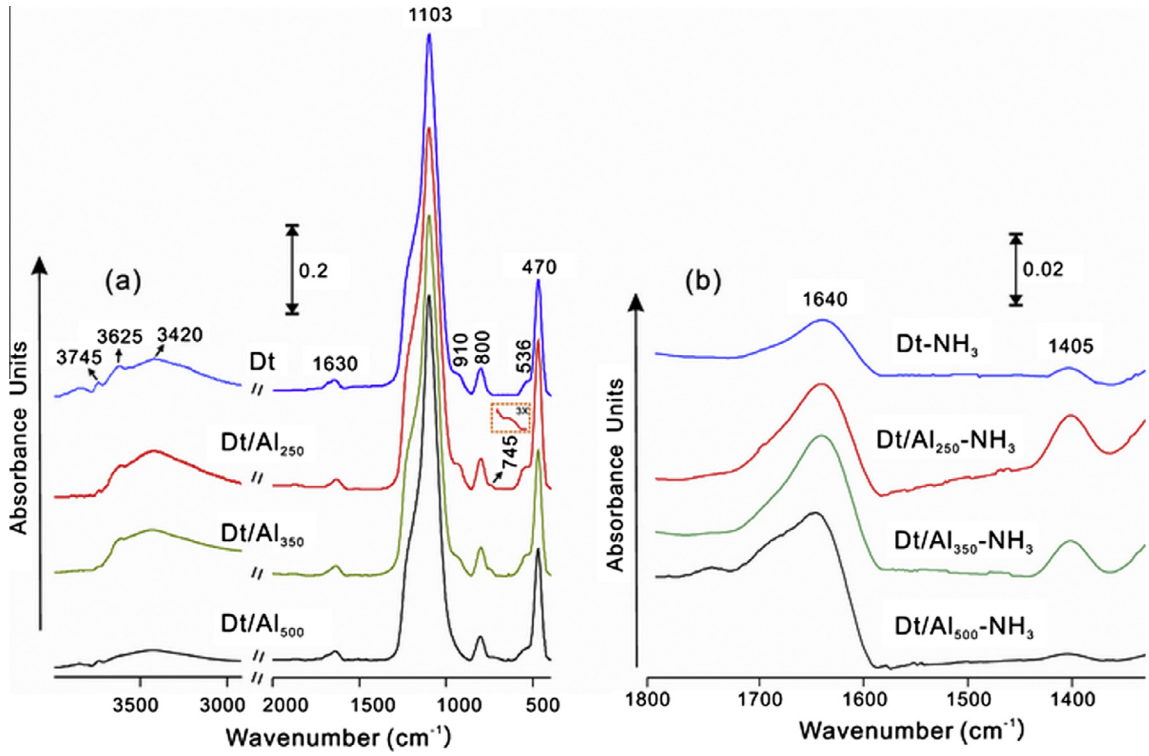

Fig. 3. FTIR spectra of diatomite and Al-incorporated diatomite obtained at various heating temperatures (insert: 3 times magnified band signals) (a) before and (b) after NH_3 adsorption.

Al^{3+} ions can be incorporated into the SiO_4 structure of diatomite by the condensation reaction of Si-OHs and Al-OHs, as revealed by the results of the ^{29}Si MAS NMR spectrum.

3.2. Effect of Al incorporation on the solid acidity of diatomite

NH_3-FTIR analysis is applied in this study to differentiate Brønsted (B) and Lewis (L) acidity because the reaction of B and L acid sites with NH_3 results in different characteristic vibration bands. Compared with the original diatomite, several new vibration bands appeared at approximately 1640 and 1405 cm^{-1} in the FTIR spectra of NH_3-adsorbed diatomite (Fig. 3b). The 1640 cm^{-1} band is attributed to NH_3 coordinated to the Lewis acid sites (denoted as L:NH_3), and the 1405 cm^{-1} band is attributed to NH_4^+ [42]. This result indicates the coexistence of B and L acid sites in Dt. These acid sites primarily arise from the Si-OHs (B acid sites) of diatomaceous silica, Al-OHs (B acid sites) of clay mineral impurities, and unsaturated Al^{3+} ions (L acid sites) of clay minerals [9,42]. After Al incorporation and heating at 250 °C, the areas of the two characteristic bands greatly increase, indicating the appearance of new B and L acid sites. These newly appeared acid sites are attributed to the incorporated Al_{13}, which contains numerous Al-OHs and unsaturated Al^{3+} ions with B and L acidity. In contrast to Dt/Al_{250}-NH_3, the 1405 cm^{-1} band of Dt/Al_{350}-NH_3 is weakened, and the 1640 cm^{-1} band is strengthened. This finding is due to the dehydroxylation of the associated Al_{13} and the formation of γ-Al_2O_3 microcrystals, decreasing the amount of hydroxyl groups while increasing the unsaturated Al^{3+} ions, which increases the L acidity. After heating at 500 °C, Al-incorporated diatomite shows a weak band, which is due to the few hydroxyl groups of the γ-Al_2O_3 microcrystals. In addition, the newly formed unsaturated Al^{3+} ions sourced from Al_{13} dehydroxylation greatly increase the amount of L acid sites, strengthening the 1630 cm^{-1} band, as observed in the FTIR spectrum of Dt/Al_{500}-NH_3 (Fig. 3b).

The results demonstrate that the Al incorporation into the structure increases the number of acid sites, and the increase of various types of acid sites depends on the heating temperature of the Al-incorporated diatomite preparation.

4. Conclusions

In this study, Al was incorporated into the structure of diatomite by the condensation reaction of the hydroxyl groups of Al_{13} and diatomite, which greatly increased the solid acidity of diatomite. Loading and subsequent heating at various temperatures did not affect the integrated amorphous structure of diatomite, as revealed by the XRD results, but did result in a decrease of hydroxyl groups of diatomite for the condensation reaction with those of the Al_{13}. Al incorporation proceeds more readily by the condensation reaction of hydroxyl groups of Al_{13} with single silanols than by that with geminal silanols. The Al-incorporated diatomite possesses a new surface functional group, Si–O–Al(OH), resulting from the condensation reaction of Al_{13} and diatomite. The newly appeared groups change the solid acidity of diatomite and increase the number of B and L acid sites of diatomite. The improvement of acidity with the different types of sites depends on the heating temperature of the preparation process for Al-incorporated diatomite. By heating at 250 and 350 °C, the B and L acid sites increase drastically due to the Al-OH content of the incorporated Al_{13}; however, by heating at 500 °C, the newly appeared B acid sites disappear and transform to L acid sites via the dehydroxylation of Al_{13}, and the number of L acid sites dramatically increases.

These fundamental results provide the empirical evidence and the new insight for the proposal that Al can be incorporated into the structure of diatom shell and post-mortem enrichment of Al naturally occurs [26,22,34]. Moreover, the influence of Al incorporation on the surface properties (surface solid acidity) of diatomite

is firstly investigated: the solid acidity is tuneable by heating and L acid sites appear in the diatom shell which was proposed to possess only B acid sites [43]. Rich solid acid sites of Al-incorporated diatomite are promising for applications as solid acid catalysts.

It is noteworthy that Al incorporation into silica texture of zeolite by isomorphous substitution has been widely accepted [44,45]. Whether can Al be incorporated into the structure of diatomite by substitution? We are focusing on it.

Acknowledgments

The financial supports from the National Natural Scientific Foundation of China (Grant No. 41202024), National Key Technology Research and Development Program of the Ministry of Science and Technology of China (Grant No. 2013BAC01B02) and Science and Technology Program of Guangzhou, China (Grant No. 201510010138) are gratefully acknowledged. This is a contribution (No. IS-2124) from GIGCAS.

Appendix A. Supplementary material

Supplementary data associated with this article can be found, in the online version, at http://dx.doi.org/10.1016/j.jcis.2015.08.058.

References

[1] P. Yuan, H.P. He, D.Q. Wu, D.Q. Wang, L.J. Chen, Spectrochimica Acta Part A – Molecular and Biomolecular Spectroscopy 60 (2004) 2941–2945.
[2] D. Losic, J.G. Mitchell, N.H. Voelcker, Adv. Mater. 21 (2009) 2947–2958.
[3] D. Liu, P. Yuan, D.Y. Tan, H.M. Liu, T. Wang, M.D. Fan, J.X. Zhu, H.P. He, J. Colloid Interface Sci. 388 (2012) 176–184.
[4] D. Liu, W.W. Yuan, L.L. Deng, W.B. Yu, H.J. Sun, P. Yuan, J. Colloid Interface Sci. 424 (2014) 22–26.
[5] W. Tsai, K. Hsien, J. Yang, J. Colloid Interface Sci. 275 (2004) 428–433.
[6] M. Al-Ghouti, M. Khraisheh, M. Ahmad, S. Allen, J. Colloid Interface Sci. 287 (2005) 6–13.
[7] H. Hadjar, B. Hamdi, M. Jaber, J. Brendlé, Z. Kessaïssia, H. Balard, J.B. Donnet, Microporous Mesoporous Mater. 107 (2008) 219–226.
[8] F. Chang, J. Qu, H. Liu, R. Liu, X. Zhao, J. Colloid Interface Sci. 338 (2009) 353–358.
[9] D. Liu, P. Yuan, D. Tan, H. Liu, M. Fan, A. Yuan, J. Zhu, H. He, Langmuir (2010).
[10] P. Yuan, D. Liu, M. Fan, D. Yang, R. Zhu, F. Ge, J.X. Zhu, H. He, J. Hazard. Mater. 173 (2010) 614–621.
[11] M.S. Aw, S. Simovic, J. Addai-Mensah, D. Losic, Nanomedicine 6 (2011) 1–15.
[12] P. Yuan, D. Liu, D.Y. Tan, K.K. Liu, H.G. Yu, Y.H. Zhong, A.H. Yuan, W.B. Yu, H.P. He, Microporous Mesoporous Mater. 170 (2013) 9–19.
[13] J.C. Lewin, Geochim. Cosmochim. Acta 21 (1961) 182–198.
[14] A.J. Van Bennekom, J.H. Fred Jansen, S.J. van der Gaast, J.M. van Iperen, J. Pieters, Deep Sea Research Part A. Oceanographic Research Papers 36 (1989) 173–190.
[15] S. Dixit, P. Van Cappellen, A.J. van Bennekom, Mar. Chem. 73 (2001) 333–352.
[16] P. Van Cappellen, S. Dixit, J. van Beusekom, Global Biogeochem. Cycles 16 (2002).
[17] P. Van Cappellen, S. Dixit, M. Gallinari, Biogeochemical Silicium Cycle: Elemental to Global Scale, vol. 28, 2004, pp. 417–454.
[18] D.C. Hurd, Earth Planet. Sci. Lett. 15 (1972) 411–413.
[19] D.C. Hurd, F. Theyer, Adv. Chem. Ser. (1975) 211–230.
[20] D.C. Hurd, C. Wenkam, H.S. Pankratz, J. Fugate, Science 203 (1979) 1340–1343.
[21] D.C. Hurd, H.S. Pankratz, V. Asper, J. Fugate, H. Morrow, Am. J. Sci. 281 (1981) 833–895.
[22] E. Koning, M. Gehlen, A.M. Flank, G. Calas, E. Epping, Mar. Chem. 106 (2007) 208–222.
[23] M. Stoffyn, Science 203 (1979) 651–653.
[24] A. Van Bennekom, A. Buma, R. Nolting, Mar. Chem. 35 (1991) 423–434.
[25] M. Gehlen, L. Beck, G. Calas, A.M. Flank, A. Van Bennekom, J. Van Beusekom, Geochim. Cosmochim. Acta 66 (2002) 1601–1609.
[26] E. Koning, E. Epping, W. Van Raaphorst, Aquat. Geochem. 8 (2002) 37–67.
[27] S.M. Holmes, B.E. Graniel-Garcia, P. Foran, P. Hill, E.P.L. Roberts, B.H. Sakakini, J. M. Newton, Chem. Commun. (2006) 2662–2663.
[28] F. Noll, M. Sumper, N. Hampp, Nano Lett. 2 (2002) 91–95.
[29] D. Losic, K. Short, J.G. Mitchell, R. Lal, N.H. Voelcker, Langmuir 23 (2007) 5014–5021.
[30] D.J. Hydes, Science 205 (1979) 1260–1262.
[31] S.B. Moran, R.M. Moore, Nature 335 (1988) 706–708.
[32] S.B. Moran, R.M. Moore, Geochim. Cosmochim. Acta 56 (1992) 3365–3374.
[33] E.G. Vrieling, L. Poort, T.P.M. Beelen, W.W.C. Gieskes, Eur. J. Phycol. 34 (1999) 307–316.
[34] S. Loucaides, P. Michalopoulos, M. Presti, E. Koning, T. Behrends, P. Van Cappellen, Chem. Geol. 270 (2010) 68–79.
[35] H. Saalfeld, Angew. Chem. – Int. Ed. 70 (1958) 630.
[36] D.T.B. Tennakoon, J.M. Thomas, W. Jones, T.A. Carpenter, S. Ramdas, J. Chem. Soc. – Faraday Trans. I 82 (1986) 545–562.
[37] M.L. Occelli, A. Auroux, G.J. Ray, Microporous Mesoporous Mater. 39 (2000) 43–56.
[38] P. Yuan, D.Q. Wu, Z.Y. Lin, G.Y. Diao, J.L. Peng, J.F. Wei, Spectrosc. Spect. Anal. 21 (2001) 783–786.
[39] P. Yuan, D. Liu, M.D. Fan, D. Yang, R.L. Zhu, F. Ge, J.X. Zhu, H.P. He, J. Hazard. Mater. 173 (2010) 614–621.
[40] J. Madejova, P. Komadel, Clays Clay Miner. 49 (2001) 410–432.
[41] V.C. Farmer, Infrared Spectra of Minerals, Mineralogical Society (1974).
[42] D. Liu, P. Yuan, H. Liu, J. Cai, Z. Qin, D. Tan, Q. Zhou, H. He, J. Zhu, Appl. Clay Sci. 52 (2011) 358–363.
[43] P. Yuan, D.Q. Wu, H.P. He, Z.Y. Lin, Appl. Surf. Sci. 227 (2004) 30–39.
[44] S. BongáHong, Chem. Commun. (1996) 425–426.
[45] O.H. Han, C.S. Kim, S.B. Hong, Angew. Chem. Int. Ed. 41 (2002) 469–472.